Morphological Alterations Induced by Temperature and Humidity in Ethylene−Vinyl Alcohol Copolymers

Amparo López-Rubio,[†] Jose M. Lagaron,*[,†] Enrique Giménez,[‡] David Cava,[†] Pilar Hernandez-Muñoz,[†] Tomoyuki Yamamoto,[§] and Rafael Gavara[†]

Packaging Lab., Institute of Agrochemistry and Food Technology, CSIC, Apdo. Correos 73, E-46100 Burjassot, Spain; Dpto. of Technology, University Jaume I, Campus Riu Sec, Castellon E−12071, Spain; and Central Research Laboratory, The Nippon Synthetic Chemical Industry Co., Ltd. (NIPPON GOHSEI), 13-1, Muroyama 2-chome, Ibaraki, Osaka 567-0052, Japan

Received September 10, 2003; Revised Manuscript Received October 19, 2003

ABSTRACT: The morphologies of a number of high barrier ethylene−vinyl alcohol food packaging films with different ethylene contents have been evaluated by simultaneous WAXS/SAXS, FT-IR, DSC, and Raman spectroscopy. This rather descriptive pioneering study was aimed at the understanding of the morphological changes that occur in these polymers as a result of temperature, humidity, and combination of temperature and humidity treatments. From the results, the temperature effect was, as expected, found to improve polymer crystalline morphology, leading to a higher, denser, and more stable crystallinity. Lower ethylene content copolymers underwent partial solid−solid phase transition toward a more thermodynamically stable monoclinic morphology upon sufficient annealing. On the other hand, moisture sorption was found to result in melting of ill-defined crystals, particularly for the lowest ethylene content copolymers. This water sorption-induced crystal melting process has not been reported before and was seen to be largely suppressed by enhancing crystal stability. Combined temperature and humidity effects, as those for instance generated in retorting autoclaves, were found to dramatically deteriorate the polymer crystallinity, irrespective of initial crystal robustness. By making use of simultaneous time-resolved WAXS/SAXS experiments during in-situ retorting of a water-saturated EVOH copolymer with 32 mol % of ethylene, it was found that heated moisture weakened very readily the polymer crystalline morphology, which melted around 80 °C below its actual melting point.

Introduction

Ethylene−vinyl alcohol copolymers are a family of random semicrystalline materials with excellent barrier properties to gases and hydrocarbons and with outstanding chemical resistance.[1] EVOH copolymers are commonly produced via a saponification reaction of a parent ethylene-*co*-vinyl acetate copolymer, whereby the acetoxy group is converted into a secondary alcohol. These materials have been increasingly implemented in many pipe and packaging applications where stringent criteria in terms of chemical resistance and in gas, water, aroma, and hydrocarbon permeation are to be met. In particular, the copolymers with low contents of ethylene (below 38 mol % ethylene) have outstanding barrier properties, under dry conditions, compared to other polymeric materials. The crystalline morphology of these copolymers is relatively well-known across composition and has been the subject of two previous studies.[2,3]

An important application of these materials is as barrier layer in multilayer structures to be used in various packaging designs for foodstuffs. The presence of EVOH in the packaging structure is key to food quality and safety because it reduces the ingress of oxygen and the loss of aroma components during extended package shelf life. Despite the low gas permeation, EVOH copolymers generally show poor moisture resistance. The appetite for water of these materials, which results in a high water uptake, leads to deterioration of the gas barrier performance in high relative humidity environments.[4] This deterioration is thought to derive from the fact that the inter- and intramolecular hydrogen bonding (so-called self-association) provided by the hydroxyl groups is intercepted by water molecules. This interaction strongly reduces interchain cohesion and mechanical integrity and increments the fractional free volume of the polymer (plasticization effect) for the permeants to travel across polymer packages. The plasticizing effect of water on the barrier properties of EVOH is time-dependent, especially if the hydrophilic layer is protected by a water barrier such as polypropylene as in the case of packages for food retorting. When such retortable packs (containing aqueous foodstuffs) are subjected to steam retorting, water passing through the protective hydrophobic layer is thought to be sorbed on the EVOH layer in such quantities that the barrier layer becomes quite permeable to oxygen. The rate of water release through the outer polypropylene layer becomes very slow on cooling, so the oxygen permeability can remain elevated for many weeks.[5] Tsai and Jenkins[6] reported that the oxygen barrier of retortable packages containing an EVOH barrier layer was initially reduced by 2 orders of magnitude when these containers were subjected to steam or pressurized water during thermal processing, and during long-term storage (>200 days) the barrier was partially recovered (by a factor of 10).

Despite the extensive characterization of the effects on barrier properties that humidity and combined temperature and humidity environments can have on these materials, there is very little understanding of the actual morphological consequences. Yet, only a sound knowledge about these morphological effects can help

[†] Institute of Agrochemistry and Food Technology.
[‡] University Jaume I.
[§] The Nippon Synthetic Chemical Industry Co., Ltd.
* To whom correspondence should be addressed. E-mail: lagaron@iata.csic.es.

10.1021/ma035346j CCC: $25.00
Published on Web 11/20/2003

designing appropriate and effective strategies to protect the materials from undesirable property damages. In this context, the main aim of this novel study is to shed light onto the fundamentals of the structural changes that occur in these copolymers upon direct exposure to (i) thermal treatments, (ii) moisture sorption, and (iii) combination of temperature and humidity, i.e., during retorting processes.

Experimental Section

Materials. Six different commercial ethylene−vinyl alcohol copolymer grades (Soarnol) supplied by The Nippon Synthetic Chemical Industry Co., Ltd. (NIPPON GOHSEI) (Japan), were analyzed: EVOH26, EVOH29, EVOH32, EVOH38, EVOH44, and EVOH48, where the number indicates the mole percentage of ethylene in the copolymer composition.

Two types of sample morphologies were used in the present work: (i) Coextruded EVOH films (ca. 10 μm thickness) between polypropylene layers with no adhesive for easy delamination of the high barrier layer prepared at NIPPON GOHSEI and (ii) compression-molded plates (ca. 1 mm thickness) obtained by both rapid cooling (quenched in water) to mimic extrusion conditions on crystalline morphology and slow cooling (15 °C/min) from the melt to obtain a more thermodynamically stable crystalline morphology. Samples were, unless otherwise stated, dried at 70 °C in a vacuum during a week before undergoing testing. The reason for studying extruded thin film samples is that most food packaging applications of these materials are presented in this form.

Methods. The materials were thermally treated under dry and humid conditions in a conventional oven (annealing) and in a sterilization autoclave (retorting), respectively.

DSC experiments were carried out in a Perkin-Elmer DSC-7 calorimeter. The heating and cooling rate for the runs was 10 °C/min, the typical sample weight being around 8 mg. Calibration was performed using an indium sample. All tests were carried out, at least, in duplicate.

Raman measurements were carried out with an NIR-FT-Raman Perkin-Elmer Spectrum 2000 instrument equipped with a diode pumped Nd:YAG laser PSU with a spectral resolution of 2 cm^{-1}. Transmission FT-IR experiments were recorded under a N_2-purged environment with a Bruker Tensor 37 equipment with 1 cm^{-1} resolution.

Simultaneous WAXS and SAXS experiments were carried out at the synchrotron radiation source in the polymer beam A2 at Hasylab (DESY) in Hamburg (Germany). Scattering patterns were recorded using a one-dimensional detector and an incident radiation wavelength, λ, of 0.15 nm. WAXS and SAXS data were corrected for detector response and beam intensity and calibrated against PET and rat tail standards, respectively. Determination of the long period was derived from background-subtracted and Lorentz-corrected SAXS data.[7] Temperature scans were also carried out at 5 °C/min on dry (sandwiched between aluminum foil) and in water saturation conditions for EVOH32 films. Water saturation conditions during the temperature experiment were ensured by sealing a water-saturated specimen in excess of moisture between "Kapton" polyimide films and O-rings rubber seals inside typical screwed rectangular cell compartments designed for measuring liquids as a function of temperature, available at the station.[8] Experiment success was checked by observation of constant background intensity over the experiment and presence of moisture in the cell after termination of the thermal experiments, which indicated that moisture did not leak off the cell during the temperature run. The cited conditions are thought to closely simulate circumstances occurring during industrial retorting processes.

Results and Discussion

Temperature Effect. Figure 1 shows WAXS and SAXS (as inset) patterns of the EVOH26 film after annealing for 20 min at different temperatures. These

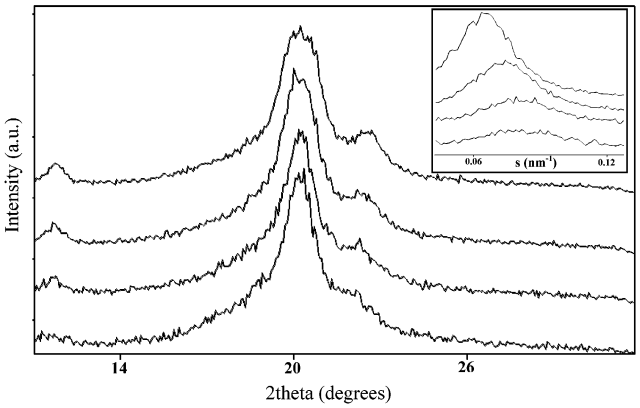

Figure 1. WAXS and SAXS raw patterns (inset) of annealed for 20 min EVOH26 at, from bottom to top, 100 (dry sample), 120, 135, and 160 °C.

annealing steps reproduce potential retorting conditionings given to these materials but without the water vapor factor. From this Figure 1, a progressive strengthening of the WAXS crystalline and SAXS patterns and a shift to higher repeat distances of the SAXS peak maximum can be seen upon increasing annealing temperature. In fact, the crystalline morphology is seen to partially evolve from a defective orthorhombic morphology, a result of crash cooling, toward the monoclinic unit cell typical of the slow cooled material[2] and thermodynamically more stable.

This kinetically slow thermally induced solid−solid phase transition evolution is more clearly revealed at the highest annealing temperatures by both broadening of the (110) reflection and shift to higher angle of the (200) reflection and has been reported before upon annealing of an EVOH32 sample during sufficient time at relatively high temperature.[9] The above phase transformation evolution was only observed for EVOH26, EVOH29, and less clearly for EVOH32, the other samples remaining orthorhombic throughout annealing. The broadening of the (110) reflection is, in this case, due to early splitting of this into the two monoclinic reflections (110) and$(1\bar{1}0)$. These changes in the crystalline morphology cannot be observed during a typical temperature scan of the samples, even at the relatively slow ramp speed of 5 °C/min (see later in text), because of its rather slow kinetics. Quantification of crystallinity was attempted in compression-molded specimens but is not shown due to difficulties in setting a soundly justified position during curve fitting for the amorphous halo. The complex issue of rigorous crystallinity determination for these polymers will be the topic of a separate study. Nevertheless, Figure 2 shows the evolution of the unit cell parameters *a* and *b* (the *c* axis is considered to be the fiber period of the planar zigzag chain conformation and is estimated from the literature to be a constant at 2.54 Å)[2,3] and the lattice volume as a function of ethylene content and annealing temperature. The *a* and *b* axes were determined from the (200) and (110) crystallographic planes at angles ca. 22° and 21°, respectively.

From this figure, it can be observed that a contraction of the *a* axis and a small expansion of the *b* axis occurs with increasing annealing temperature, leading therefore to an overall decrease in lattice volume. These results are consistent with an improvement in crystalline morphology toward thicker and more thermody-

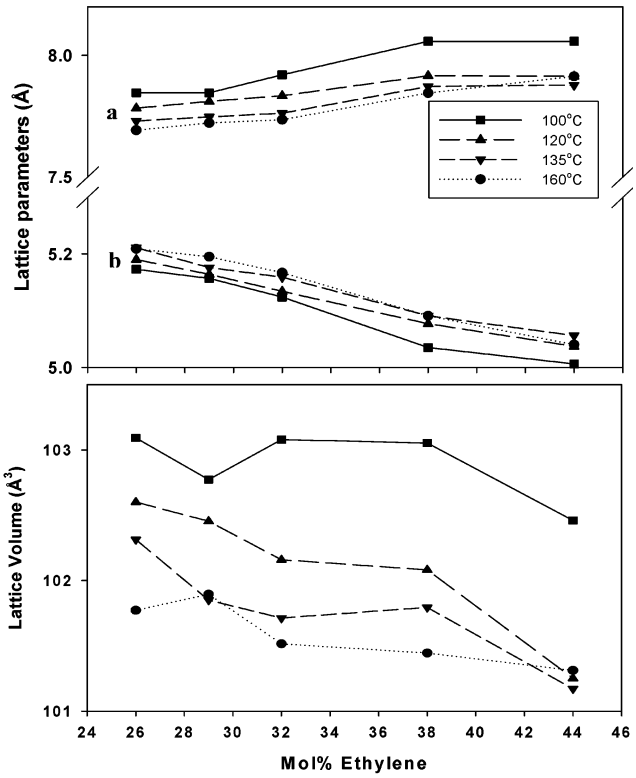

Figure 2. Evolution of *a* and *b* lattice parameters and lattice volume as a function of annealing temperature and ethylene content.

Table 1. Long Period of EVOH Films under Dry and Water Saturation Conditions

	dry (nm)	water saturated (nm)	difference
EVOH 26	10.8	13.3	2.5
EVOH 29	10.2	12.6	2.4
EVOH 32	10.0	12.7	2.7
EVOH 38	9.7	10.7	1.0
EVOH 44	10.1	10.9	0.8

namically stable crystals, in agreement with previous work.[2]

Figure 3 plots the copolymers long period as determined from SAXS data as a function of annealing temperature and ethylene content. From this figure, one

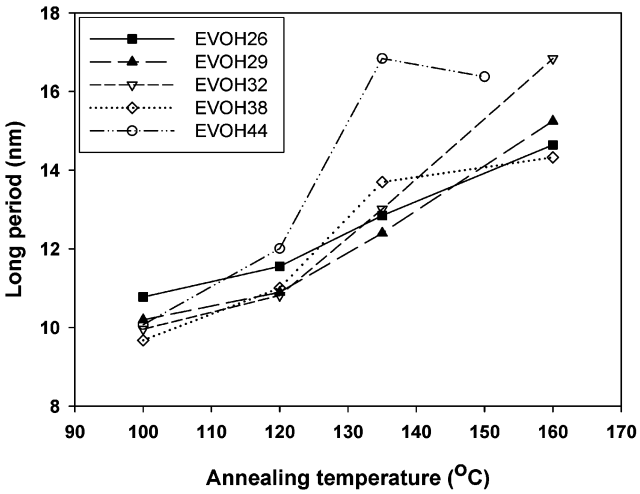

Figure 3. Long period as a function of annealing temperature for all copolymers.

can observe that the long period after annealing at 100 °C is generally longer for the lower ethylene content copolymers. The repeat distance increases with annealing temperature; this increase is larger for the high ethylene content copolymers because these materials have lower melting point (see copolymers melting point in the first column of Table 3), and therefore, annealing is comparatively more aggressive for these particular samples. These observations are consistent with a general improvement in phase morphology and crystallinity development at expenses of the disappearance of the more defective crystals, resulting in a more homogeneous and sharply defined two phase architecture. However, samples EVOH38 and EVOH44 slow down increase and decrease long period, respectively, at the highest annealing temperature due to extensive melting during annealing and subsequent fast recrystallization upon sample removal from the oven, leading again to defects.

Thus, a general picture of the expected temperature-induced improvement in crystalline morphology and of a more regular stacking of the lamellae can be drawn from the above results upon annealing. This is a very general and well-known response in crystalline polymers.

Table 2. Normalized Intensity of the 1140 cm^{-1} (by Subtracting the Absorbance of the 1333 cm^{-1} Standard Band and Multiplying by 100) FT-IR Band for the Various Materials after Various Treatments

treatment	EVOH26	EVOH29	EVOH32	EVOH38	EVOH44	EVOH48
water saturated	17	13	13	12	12	13
fully desorbed	15	14	14	13	12	13
dry at 70 °C	20	18	16	15	14	14
dry and water saturated	14	13	13	13	12	13
annealed at 120 °C	23	21	20	19	17	17
annealed at 160 °C[a]	30	29	25	24	19	18
annealed at 160 °C and water saturated[a]	29	28	25	25	20	19

[a] EVOH44 and EVOH48 were annealed at 150 °C instead of at 160 °C.

Table 3. DSC Maximum of Melting (T_m), Melting Enthalpy (ΔH), and Peak Width at the Base of Crash-Cooled and Retorted Crash-Cooled Specimens

	untreated			120 °C, 20 min, autoclave			difference		
	T_m (°C)	ΔH (J/g)	width (°C)	T_m (°C)	ΔH (J/g)	width (°C)	ΔT_m (°C)	$\Delta(\Delta H)$ (J/g)	Δwidth (°C)
EVOH 26	200.1 ± 0.2	90.6 ± 13	16.8 ± 0.5	193.2 ± 0.1	96.0 ± 0.3	23.6 ± 2.6	−6.9	5.5	6.8
EVOH 29	194.9 ± 0.1	86.6 ± 4.4	17.8 ± 0.4	189.8 ± 1.0	85.1 ± 2.5	17.2 ± 0.1	−5.1	−1.5	−0.7
EVOH 32	187.0 ± 0.1	83.5 ± 0.1	13.6 ± 5.4	183.3 ± 4.0	82.2 ± 4.7	22.0 ± 0.3	−3.7	−1.3	8.4
EVOH 38	178.9 ± 1.2	83.4 ± 20	16.6 ± 4.4	174.3 ± 0.4	86.6 ± 1.5	19.2 ± 5.8	−4.6	3.2	2.6
EVOH 44	167.3 ± 0.1	84.6 ± 6.0	17.5 ± 0.1	165.7 ± 1.4	83.0 ± 12	20.1 ± 3.8	−1.7	−1.6	2.7
EVOH 48	160.3 ± 0.3	72.9 ± 25	13.9 ± 0.7	158.5 ± 3.3	72.6 ± 6.0	16.5 ± 0.7	−1.8	7.9	2.6

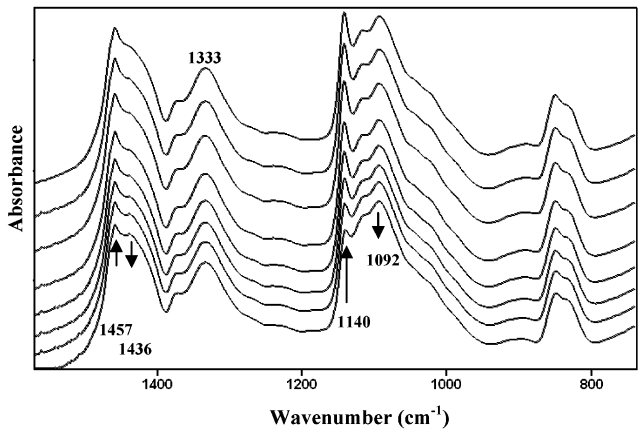

Figure 4. FT-IR spectra in the range 700−1600 cm^{-1} of annealed for 20 min EVOH32 film at, from bottom to top, 70, 100, 120, 130, 140, 150, 160, and 170 °C.

Further substantiation of these effects was alternatively gained by FT-IR experiments. From the results that follow, the FT-IR technique is uncovered as an extremely valuable characterization tool for these materials. The reasons being the high sensitivity of the technique to simultaneously detect changes in crystallinity and water sorption levels. Figure 4 shows the effect of a stepwise annealing process on the infrared spectrum of an EVOH32 specimen. In this figure, the arrows indicate changes in the absorbance of some bands of interest with increasing temperature. To obtain the figure, a single specimen of the sample was cumulatively annealed at the various temperatures directly onto the FT-IR sample holder (to avoid changes in samples thickness or optical path), and between annealing steps, it was taken out of the oven and FT-IR recorded. From the experiments, it can be observed that, upon annealing of this sample, a large increase in intensity of a band positioned at ca. 1140 cm^{-1} becomes evident. Interestingly, the band at 1333 cm^{-1} did not modify its intensity during the process and can, therefore, be potentially used as an internal standard during further experiments of this kind. A broad envelop peaked at 1092 cm^{-1} was seen to decrease intensity because it hides the contribution of at least an amorphous band at ca. 1115 cm^{-1}.

The 1140 cm^{-1} band (likely assigned to C−O−C or to C−C coupled with a CO stretching mode)[10,11] is known from previous works[11,12] to arise from all-trans conformation crystallizable chain segments and is confirmed to be so throughout this work. Although in principle all-trans conformers could be placed anywhere within the sample (as they are only ascribed to one-dimensional order along the polymer chain), the vast majority of these must, to a good approximation, be within a crystalline environment for unstretched semicrystalline polymer samples annealed (during drying) above T_g.

Despite the fact that the coextrusion process may lead to some preferential orientation of the EVOH film in the machine direction, this was not observed, by sample rotation, to affect the present FT-IR measurements throughout the work. Figure 5 shows more clearly the changes in the absolute absorbance of this band with annealing temperature. From this figure, it can be seen that the molecular order along the chain improves as the intensity of this band rises continuously with increasing annealing temperature. Note, however (thicker line in Figure 5), that annealing at the higher temperature (170 °C) results in a slight decrease of molecular order, in line with analogous SAXS observations in Figure 3 for EVOH38 and EVOH44 at the highest temperatures. FT-IR becomes thus an excellent tool to ascertain phase structure modifications in molecular order, throughout the use of the 1140 cm^{-1} band, for these particular materials.

Of particular relevance is also the inset in Figure 5, showing some changes of the OH stretching band upon stepwise annealing. From this figure, it is learned that as annealing temperature is increased, a decrease in band absorption occurs up to about 150 °C. Further annealing at higher temperatures does not lead to band shape or intensity modifications. A feasible explanation for this particular behavior is the progressive loss of remnant moisture present in the sample. Previous experiments by TGA suggested that some water molecules are very strongly linked to the polymer via hydrogen bonding, and therefore, to ensure an effective drying process, a severe thermal treatment should be applied.[9] From the experiments being described in this study, there appears to be a close interrelation between temperature, molecular order, and humidity (see later

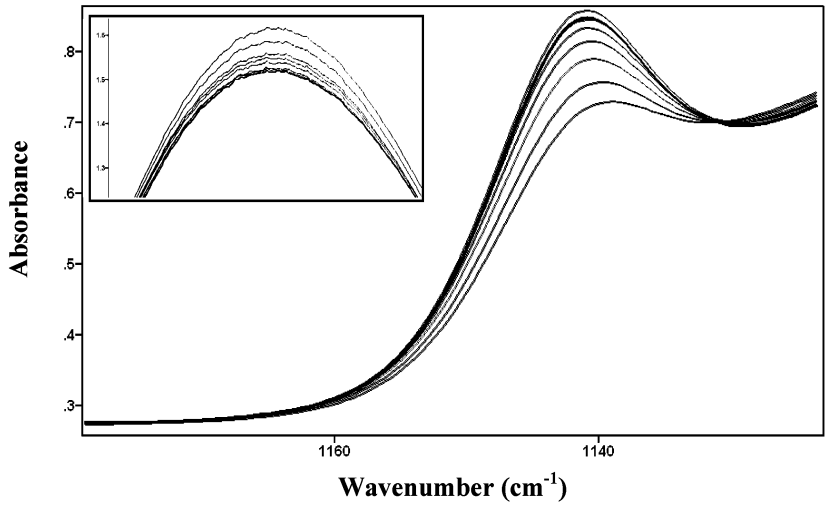

Figure 5. Absolute absorbance of the 1140 cm^{-1} FT-IR band of annealed for 20 min EVOH32 specimen at, from lower to higher absorbance, 70, 100, 120, 130, 140, 150 (overlap with 170 °C), 170 (thicker line), and 160 °C. Inset is the OH stretching band at 3347 cm^{-1} in reverse temperature order.

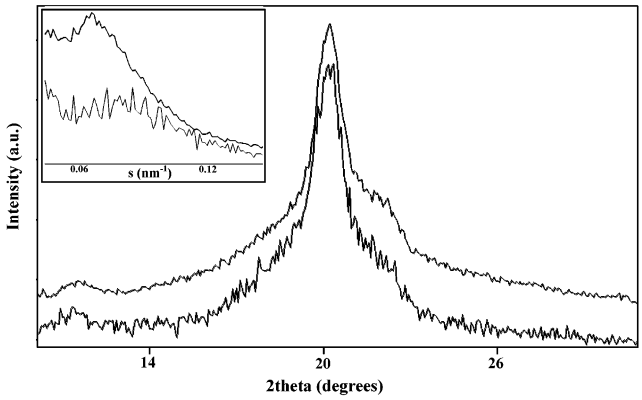

Figure 6. WAXS (normalized in intensity and shifted in the ordinate axis for comparison purposes) and raw SAXS patterns (inset, also slightly shifted in the ordinate axis) of EVOH32 dry (bottom) and saturated in water (top).

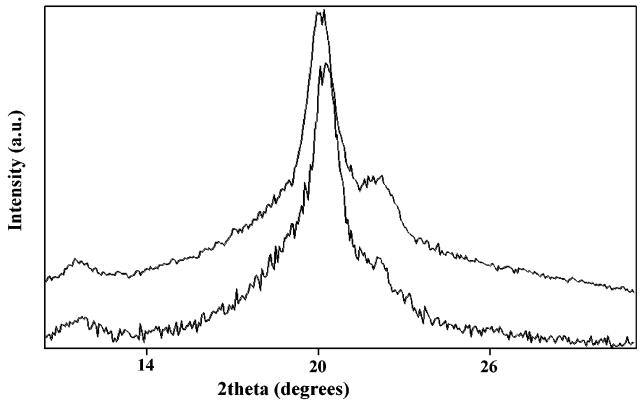

Figure 7. WAXS patterns (normalized in intensity and shifted in the ordinate axis for comparison purposes) of a film of EVOH26 dry (bottom) and water saturated (top).

in text). From a fundamental point of view, to unleash these three effects appears to be virtually impossible, and this is, therefore, one of the main outcomes arising from the results as the paper develops.

Humidity Effect. Sorption of water is known to have a severe plasticizing effect on the properties of these hydrophilic copolymers, particularly for the higher vinyl alcohol content copolymers. Most previous studies dealing with the characterization of moisture impact have measured macroscopic properties like mechanical and barrier properties, and therefore, there is a lack of morphological information on the effect of moisture sorption for these polymers.[1,4,9,12−15] Figure 6 shows the WAXS diffraction patterns of a dry (in a vacuum at 70 °C for a week) film specimen of EVOH32 and of a specimen equilibrated at 100% relative humidity (RH).

Figure 6 shows that the (200) diffraction plane at angle ca. 22° appears to resolve better upon moisture sorption. The inset in Figure 6 shows the raw SAXS patterns for these samples. From this, one can observe that the water-saturated sample exhibits a more enhanced and shifted to lower angle peak maximum. The enhancement in intensity caused by the presence of moisture could be attributed to an increase in phase contrast (scattering invariant is proportional to the square of the density contrast between amorphous phase and crystalline lamellae) due to the presence of the plasticizing moisture in only the amorphous phase. Table 1 gathers the estimated long period for all dry and moisture-saturated copolymers. From this, moisture sorption leads to an increased long period, which is generally larger for lower ethylene content copolymers.

Figure 7 shows the WAXS patterns of dry and water-equilibrated specimens of EVOH26. From this figure a more clear strengthening and shift to higher angle of the (200) orthorhombic plane than in Figure 6 can be seen. This effect on the (200) reflection is most clearly seen for EVOH26 and less clearly observed for EVOH38 and EVOH44. Calculations of lattice parameters for the diffractogram in Figure 7 indicate that the *a* axis does indeed contract from 7.85 to 7.82 Å upon water equilibrium sorption. However, the *b* axis expands from 5.17 to 5.24 Å, leading to an overall lattice volume expansion of about 1%. Contraction of the *a* axis and slight expansion of the *b* axis were indicative upon annealing in Figure 2 of progression of the crystalline phase toward a more thermodynamically stable morphology. Thus, the observations reported here appear to indicate

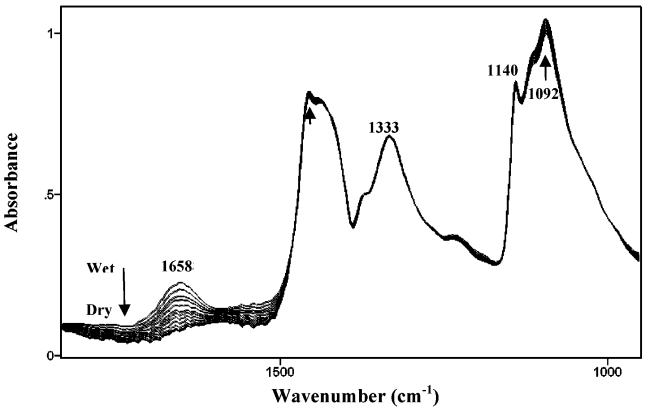

Figure 8. FT-IR spectra taken during desorption of a water equilibrated film of EVOH26. Arrows indicate the absolute absorbance changes upon water desorption. Note that this particular sample was not vacuum-dried at 70 °C before equilibrated in water.

that moisture sorption leaves a more stable arrangement of the lattice chains but with a slightly increased cell volume for this sample. However, does this imply that higher molecular order is attained upon water sorption?

To give an answer to the above question, further experiments were also carried out by FT-IR on dry samples before and after water saturation. To do that, however, a prior knowledge on the effect of moisture over the FT-IR spectrum is needed. This was derived by immersion in a 100% RH environment of specimens (not dried) of the various samples. After equilibrium sorption, these specimens were removed from the humidity conditions, wiped up the surface, and then measured by FT-IR, in-situ, during water desorption within the N_2-purged FT-IR chamber (see Figure 8).

Under these conditions, one can interpret absolute spectral modifications in the samples without interference from changes in thickness and optical path. Figure 8 shows the progressive decrease of the 1658 cm^{-1} in-plane OH bending water band upon desorption. During this process, the band at 1333 cm^{-1} remains completely unmodified, and it is, therefore, further confirmed as an adequate internal standard for the experiments displayed here. The crystallinity band at 1140 cm^{-1} also remains largely unmodified during desorption (see second and third rows in Table 2). However, the bands envelope with a maximum at 1092 cm^{-1} (having amorphous contributions)[11] appears to increase as moisture

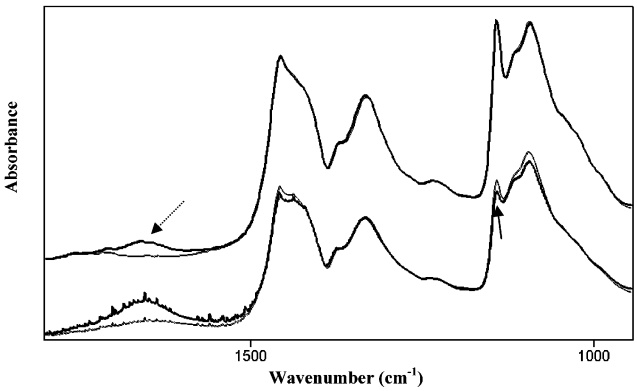

Figure 9. FT-IR spectra of EVOH26 dry at 70 °C and dry and then water saturated (thicker spectrum) at the bottom and annealed at 160 °C and water saturated after annealing at 160 °C (thicker spectrum) at the top. Continuous arrow points to the 1140 cm^{-1} crystallinity band, and discontinuous arrow points to the 1658 cm^{-1} OH in-plane bending of water.

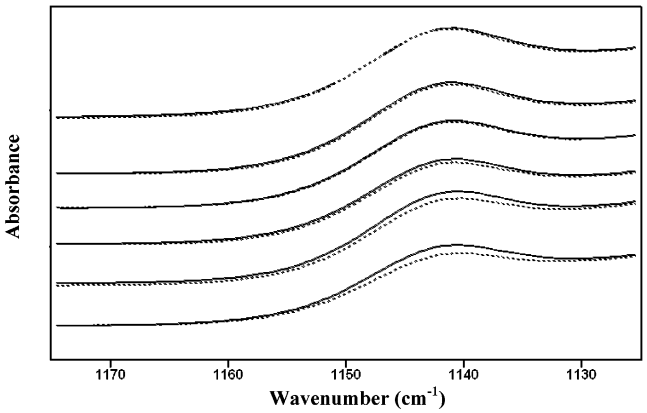

Figure 10. FT-IR spectra showing the 1140 cm^{-1} crystallinity band of annealed for 20 min at, from top to bottom, 140, 130, 120, 110, 90, and 80 °C EVOH26 specimens before (continuous) and after water saturation (discontinuous).

diffuses out of the sample, perhaps as a result of differences in absorption coefficients between dry and wet conditions for some of the corresponding modes in the amorphous phase.

With the above in mind, vacuum-dried specimens of the different samples were measured by FT-IR before and after water saturation (see two bottom spectra in Figure 9 for EVOH26). The continuous arrow in Figure 9 indicates that water sorption in EVOH26 leads to a clear (larger than the changes seen in Figure 8) band decrease of the 1140 cm^{-1} crystallinity band. This is confirmed by observation of the data in Table 2. The fourth and fifth rows in Table 2 gather the normalized absorbance of the 1140 cm^{-1} band of a dry specimen before and after water saturation for all copolymers. From this table, a crystallinity drop is found for the other copolymers, with a tendency for this to be lower in the highest ethylene content materials. Consequently, a partial dissolution of crystallinity is clearly happening for these samples upon water uptake, which from observation of Figure 8 and Table 2 is not recovered upon subsequent desorption.

Table 2 shows that, upon water desorption of the as-received materials equilibrated in water (therefore not previously dried), the intensity of the 1140 cm^{-1} crystallinity band does not appear to have a clear trend with composition or to change to a significant extent. It is worth noting that the absolute absorbances of the 1140 cm^{-1} and internal standard bands are different for different copolymers, and as a result, the normalized intensity of the crystallinity band, although it approaches them all, is not necessarily comparable between different materials. Consequently, the numbers in Table 2 can only be compared in relative terms along columns (between treatments) and not across columns (between materials). After vacuum-drying of the as-received samples, all the materials increase crystallinity (compare second and fourth rows in Table 2) due to the mild annealing treatment at 70 °C given to them for a week. When the dry samples are equilibrated in water, there is a clear decrease in crystallinity for all copolymers, especially for the lowest ethylene content samples.

An interesting question rises, however, from these observations. If sorption of water molecules leads to some reduction in crystallinity in fast cooled extruded EVOH specimens having a defective crystalline morphology, would this effect reproduce on an annealed sample when undergoing water sorption? In other words, does crystal density and morphology matter in terms of moisture resistance? This question brings in another concern: Is the 1140 cm^{-1} band drop observed by FT-IR upon moisture sorption in Figure 9 and Table 2 a true crystallinity reduction, or is it just a result of the disappearance (due to moisture plasticization) of all-trans ordered chain segments present in the amorphous phase and being held up in all-trans conformation by intermolecular hydroxyl hydrogen bonding in the glassy state?

To assess these reasonable concerns, dry specimens of the various copolymers were stepwise annealed for 20 min in an oven at various temperatures (see top spectra in Figure 9 and Table 2). By doing so, higher and more robust crystallinity is generated. Thus, similarly as in Figure 4 for EVOH32, the band at 1140 cm^{-1} ascribed to all-trans ordered conformers increases intensity with increasing annealing temperature for the copolymers, suggesting that thermally induced higher molecular order is imprinted on the materials. However, after annealing at 160 °C (150 °C for EVOH44 and 48) the samples were exposed to a 100% RH environment until equilibrium sorption and were then measured again by FT-IR at equilibrium sorption (see top spectra in Figure 9 and last row in Table 2) and during desorption inside a nitrogen-purged FT-IR chamber (results not shown). From the latter experiments, it is found that the high molecular order achieved during annealing is now not being significantly disrupted by water sorption or subsequent desorption and, therefore, rules out the hypothesis of all-trans segments relaxing in the amorphous phase due to water sorption and confirms the drop of the 1140 cm^{-1} band seen in Figure 9 and Table 2 as a genuine crystallinity destruction by dissolution.

Another supporting evidence for the above observations is the evolution of OH in-plane bending mode at 1658 cm^{-1} (pointed by a discontinuous arrow) arising from the sorbed moisture in the sample in Figure 9. This band is seen smaller in the annealed at 160 °C water-saturated sample, supporting that as annealing gives rise to a higher and more robust crystallinity in the sample the water uptake at equilibrium is clearly lower, e.g., 23% lower for EVOH26 from FT-IR measurements.

Figure 10 shows more clearly how as we increase annealing temperature of EVOH26 and, therefore, increase crystallinity and average crystalline density,

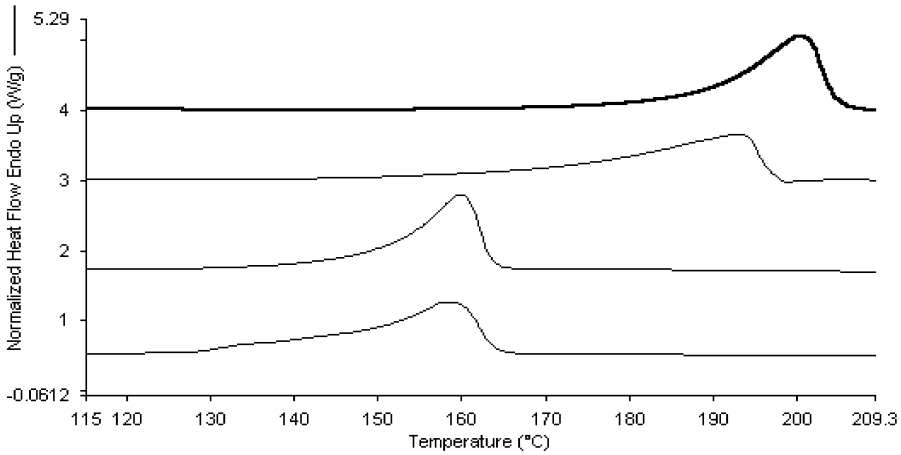

Figure 11. Melting endotherms of, from top to bottom, untreated and retorted EVOH26 and untreated and retorted EVOH48.

Table 4. DSC Maximum of Melting (T_m), Melting Enthalpy (ΔH), and Peak Width at the Base of Slow-Cooled and Retorted Slow-Cooled Specimens

	untreated			120 °C, 20 min, autoclave			difference		
	T_m (°C)	ΔH (J/g)	width (°C)	T_m (°C)	ΔH (J/g)	width (°C)	ΔT_m (°C)	$\Delta(\Delta H)$ (J/g)	Δwidth (°C)
EVOH 26	198.2 ± 0.1	94.5 ± 3.9	8.0 ± 0.1	194.3 ± 1.4	83.6 ± 1.3	19.5 ± 0.4	−3.9	−10.9	11.5
EVOH 29	193.3 ± 0.3	97.1 ± 1.9	8.4 ± 2.9	188.7 ± 3.4	91.0 ± 0.1	17.7 ± 0.1	−4.7	−6.1	9.2
EVOH 32	185.7 ± 0.7	92.8 ± 0.3	8.1 ± 6.5	186.1 ± 0.2	88.7 ± 0.5	23.5 ± 0.0	0.4	−4.1	15.4
EVOH 38	176.8 ± 0.1	91.5 ± 6.6	9.8 ± 0.6	176.1 ± 0.0	92.5 ± 10	17.3 ± 4.7	−0.8	0.9	7.5
EVOH 44	166.8 ± 0.7	91.0±5.2	10.1 ± 1.9	165.6 ± 0.6	83.7 ± 21.5	17.9 ± 3.4	−1.3	−7.3	7.8
EVOH 48	160.9 ± 0.1	86.0 ± 0.3	12.5 ± 0.3	160.3 ± 0.1	78.3 ± 0.7	15.3 ± 0.3	−0.7	−7.8	2.9

lower reduction in crystallinity is observed for this specimen after equilibrium water sorption. In fact, the annealing process at 120 °C appears to produce sufficiently stable crystals in terms of moisture resistance for this EVOH26 sample, and consequently, further annealing at higher temperatures has virtually no differentiating effect.

The overall results then suggest that water uptake leads to the dissolution of ill-defined (defective) crystallinity, most likely placed at the interphase between the crystalline lamellae and the amorphous phase. This leaves a lamellae core with improved crystalline morphology (see strengthening of the (200) plane in Figure 7) and with a slightly higher repeat distance as derived from the SAXS results due to expansion (dedensification) of the phase periodicity. The reported increase in cell volume for EVOH26 due to expansion of the *b* lattice parameter is thought to be the result of the plastizacing effect of the sorbed water in the amorphous phase, resulting in swelling stresses on the crystalline morphology.

Combined Temperature and Humidity Effect. To study the effect of the combination of the above two factors, temperature and moisture, on the morphology of EVOH copolymers, slow-cooled and crash-cooled compression-molded thicker plates were used. These samples were obtained as explained in the Experimental Section. Vacuum-dried thicker plates were used in this part because the above polymer films, typically utilized in food-packaging applications, did not withstand the treatment and irreversibly lost dimensional stability. The samples were conditioned in an autoclave at 120 °C for 20 min, typical industrial retorting conditions. It is worthy noting that in all cases treatments were carried out at temperatures well below the copolymers maximum of melting, albeit above their glass transition temperatures and around the α-relaxation temperatures.[9] The latter relaxation is picked up by dynamic-mechanical experiments and is related, by analogy to polyethylene, to relaxational motions within crystals.

From the first DSC heating scans (see Tables 3 and 4), it can be seen that the maximum of melting of the nontreated samples is higher than the melting point of the retorted samples. This is particularly the case for the copolymers with the higher vinyl alcohol contents. The samples appear, by visual inspection, to be dramatically damaged, with the presence of voids and loss of transparency, i.e., intense whitening or hazing. These effects are attributed to pressurized water vapor having penetrated the amorphous phase but also diffusing through the crystal edges and inducing partial melting and fractionation of the crystalline morphology (see later). Voiding and loss of transparency could arise from bubbles formed by water evaporation as the pressure is released rapidly after retorting in the autoclave. From the above experiments, these damaging effects do not occur upon water exposure or uptake at room temperature and evidently neither due to annealing. High temperature and humidity thus appear as a very severe aggressive combination of factors for these materials. Tables 3 and 4 gather the maximum of melting, peak width (at the base of the peak), and melting enthalpies for the various samples and conditionings recorded during the first run, and Figure 11 shows, as an example, the actual melting endotherms of crash-cooled EVOH26 and EVOH48. Although, the measured melting enthalpies (taken from the integrated area under the melting enthalpy covering from the endset of melting up to 70 °C below this) of treated and nontreated samples are only slightly smaller, pointing out that the overall degree of crystallinity may not have decreased so significantly, the melting peaks of the retorted samples have clearly broadened (particularly for the lower ethylene content samples and for the slow-cooled samples) toward lower temperature, suggesting that a more heterogeneous crystalline structure with lower

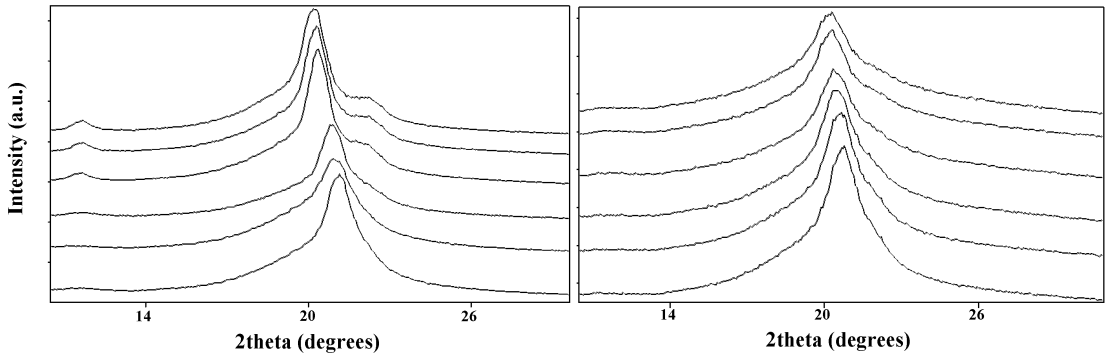

Figure 12. WAXS patterns of crash-cooled (left) and retorted crash-cooled (right) specimens of, from to top to bottom, EVOH26, EVOH29, EVOH32, EVOH38, EVOH44, and EVOH48.

crystal size and/or perfection has occurred as a result of retorting, irrespective of whether a more robust crystalline morphology (as in slow-cooled samples) was originally present. It should be noticed that the samples were dried (70 °C in a vacuum) immediately after the retorting processes and before the DSC run and that this conditioning may have to some extent reannealed the structure.

WAXS experiments were also carried out on the slow-cooled and crash-cooled retorted samples. These samples were not reconditioned after retorting to avoid reannealing and were just left to equilibrate at room temperature and 60% RH. Figure 12 shows the WAXS patterns of crash-cooled specimens before and after retorting. After retorting, the WAXS crystalline morphology has changed dramatically, particularly for the low ethylene content copolymers. The crystalline patterns are clearly less defined, and the main diffraction peak (110) at angle 20° is much broader, suggesting crystal fractionation, heterogeneity, and hence a more defective crystalline morphology. Note that Figure 1 showed also broadening of the (110) reflection at the highest annealing temperature, but there the broadening was a result of early splitting of this particular reflection into two monoclinic crystalline peaks as further suggested by a strengthening and shift toward higher angle of the (200) reflection. Similar results were found (results not shown) for slow-cooled samples, with a more stable initial crystalline morphology, suggesting that crystal robustness is not sufficient (as it was to avoid crystal dissolution during water sorption at room temperature) in terms of resistance to the process during direct exposure of EVOH to heated moisture.

Figure 13 shows the evolution of the *a* and *b* cell parameters after retorting of crash-cooled specimens as a function of ethylene content. From this figure, it can be clearly observed that retorting leads to clear expansion of the *a* (from sample EVOH26 to 38) and *b* (from sample 38 to 48) lattice parameters and, therefore, to an overall drop in crystalline density.

No pseudohexagonal crystal lattice was found as a result of any of the treatments described above as the quantity $r = (3)^{1/2}b/a$ was always larger than unity.[2] Nevertheless, retorting imposes a very strong distorting effect on the crystalline lattice morphology of the samples as further proved by Figure 14. This figure shows the Raman spectrum in the $-CH_2-$ bending range of slow-cooled EVOH29, where factor group splitting features (see arrows) characteristic of an orthorhombic lattice are seen in the untreated specimen.[16,17] After retorting, a disappearance of the orthorhombic factor group splitting patterns indicates evolution toward a very distorted orthorhombic unit cell of lower crystalline density.

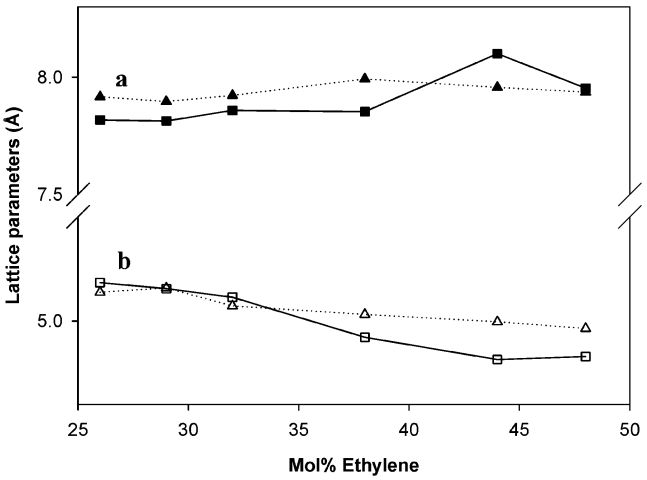

Figure 13. Evolution of lattice axis *a* and *b* of crash-cooled (squares) and retorted crash-cooled (triangles) specimens as a function of ethylene content.

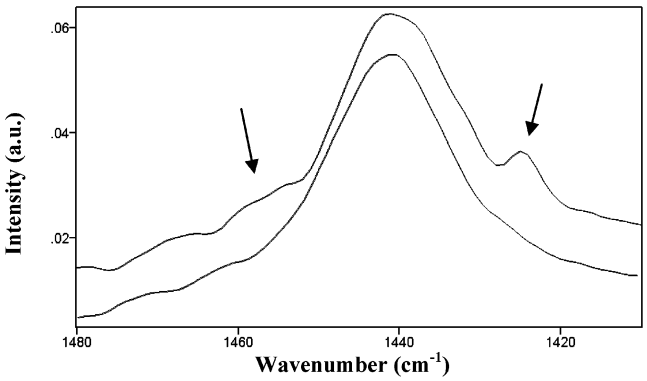

Figure 14. Raman $-CH_2-$ bending range of crash-cooled (top spectrum) and retorted crash-cooled specimens of EVOH29. Arrows indicate bands evidencing a factor group splitting effect.

From the above, it is clear that EVOH monolayers are structures that even with high thicknesses are largely susceptible to alterations during combined temperature and humidity processes and, therefore, need to be protected between hydrophobic materials in commercial applications. But what are the actual changes taking place during direct retorting of an EVOH sample? To understand the transient occurrences during this combined temperature and humidity process, a film sample of EVOH32 was scanned in temperature both

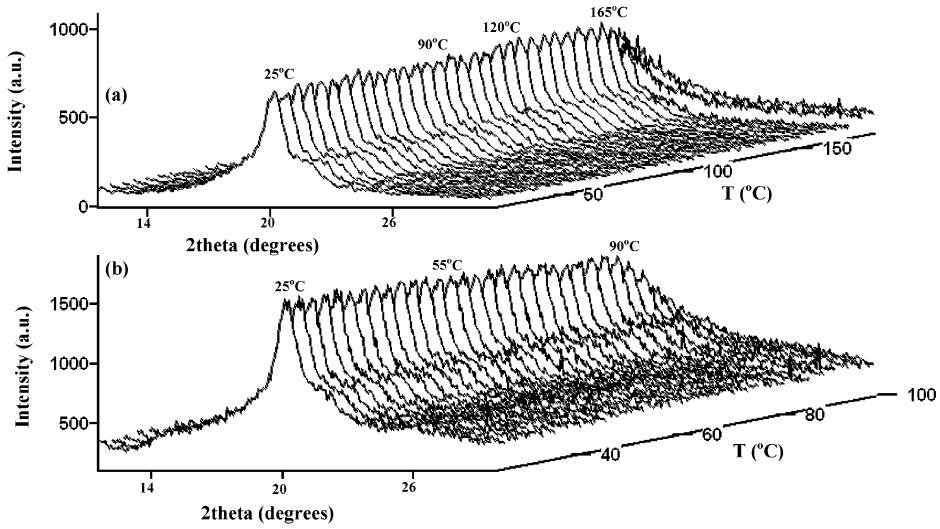

Figure 15. WAXS patterns as a function of temperature of (a) dry and (b) water-saturated EVOH32 film specimens. Note the presence in (b) of background signals underneath the crystalline EVOH patterns arising from the sample being measured in the cited liquid cell.

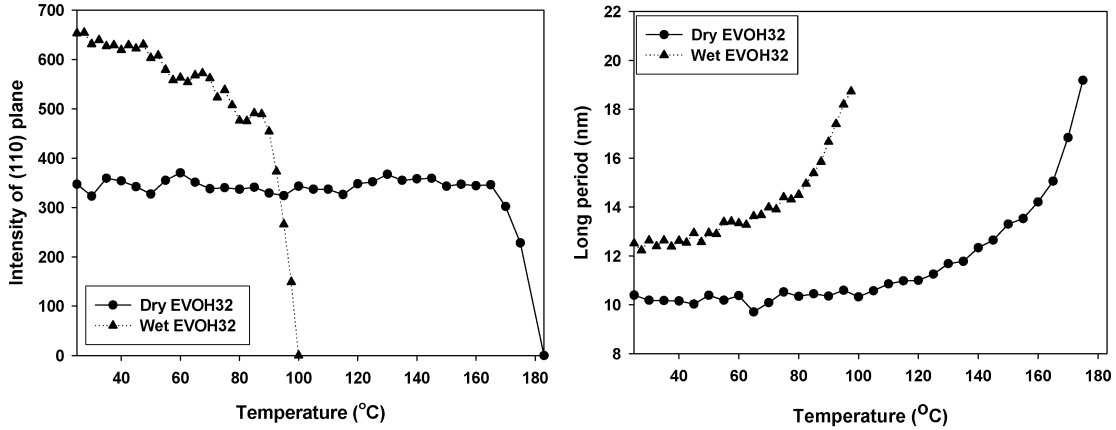

Figure 16. Intensity (left) of the (110) crystalline plane for the diffractograms plotted in Figure 15 and long period (right) as a function of temperature for a dry and water-saturated film sample.

dry and in the presence of excess saturating humidity conditions. Figure 15 shows the WAXS patterns of this sample under these conditions as a function of temperature.

From this figure, it can be seen that under dry conditions the sample retains its crystalline morphology over temperature until it reaches melting at around 183 °C, the temperature at which the crystalline patterns disappear completely in agreement with its reported melting point. On the other hand, for a water-saturated sample, the crystallinity decreases immediately above room temperature to completely disappear at around 100 °C (83 °C below its actual melting point). This is thought to be caused by pressurized heated water diffusing through thermally activated molecules within crystals, disrupting the efficient crystalline intermolecular hydrogen bonding provided by the hydroxyl groups. The crystallinity decline appears more pronounced above 50 °C and is very dramatic above 90 °C. As a result, a saturated sample of EVOH32 appears to show very little moisture resistance at temperatures immediately above 50 °C.

Figure 16 shows the evolution of the intensity of the (110) orthorhombic plane and of the long period (determined from the simultaneous SAXS patterns) with temperature. From this, it can be more clearly appreciated that under dry conditions the polymer morphology is largely retained until temperatures above 100 °C, temperature in the vicinity of the polymer α-relaxation. Beyond this temperature, the long period begins to increase shallowly up to about 160 °C and then markedly, concomitantly, the crystallinity appears to first increase slightly up to about 160 °C (annealing effect) and from then onward to decrease to a fast pace (progressive melting). On the other hand, in the wet sample the long period is relatively retained up to about 50 °C, but from there onward it progressively increases in line with the observed decease of the crystallinity up to the complete melting of the sample. The above behavior does, of course, prevent the use of EVOH as monolayer packages in commercial food retortable packaging applications. In these particular applications, only adequate multilayer structures where a dry high gas barrier EVOH layer is sandwiched between high water barrier polymers have commercial interest. In this context, a more detailed description of the combined effect of temperature and humidity on the melting and crystallization behavior of these copolymers in monolayer and multilayer structures, as well as the role of crystal stability, as a function of temperature, humidity, and composition is being currently under investigation.

Acknowledgment. The authors thank The Nippon Synthetic Chemical Industry Co. Ltd. (NIPPON GOHSEI), Japan, for financial support and Mr. Y. Saito, associate board director of Central Research Laboratory of NIPPON GOHSEI for helpful advice and suggestions during preparation of the manuscript. The work performed at the synchrotron facility in Hamburg (Hasylab, Germany) was supported by the IHP-Contract HPRI-CT-1999-00040/2001-00140 of the European Commission, and the authors acknowledge Dr. S. Funari and Mr. M. Dommach (Hasylab) for experimental support.

References and Notes

(1) Lagaron, J. M.; Powell, A. K.; Bonner, J. G. *Polym. Test.* **2001**, *20/5*, 569−577.
(2) Cerrada, M. L.; Perez, E.; Pereña, J. M.; Benavente, R. *Macromolecules* **1998**, *31*, 2559−2564.
(3) Takahashi, M.; Tashiro, K.; Amiya, S. *Macromolecules* **1999**, *32*, 5860−5871.
(4) Aucejo, S.; Catala, R.; Gavara, R. *Food Sci. Technol. Int.* **2000**, *6*, 159−164.
(5) Tsai, B. C.; Wachtel, J. A. In *Barrier Polymers and Structures*; Koros, W. J., Ed.; American Chemical Society: Washington, DC, 1990; pp 192−202.
(6) Tsai, B. C.; Jenkins, B. J. *J. Plastic Film Sheeting* **1988**, *4*, 63−71.
(7) Balta-Calleja, F. J.; Vonk, C. G. *X-ray Scattering of Synthetic Polymers*; Elsevier: Amsterdam, 1980.
(8) http://www-hasylab.desy.de/science/groups/mpikgf.
(9) Lagaron, J. M.; Gimenez, E.; Saura, J. J.; Gavara, R. *Polymer* **2001**, *42*, 7381−7394.
(10) Cooney, T. F.; Wang, L.; Sharma, S. K.; Gauldie, R. W.; Montana, A. J. *J. Polym. Sci., Part B: Polym. Phys.* **1994**, *32*, 1163−1174.
(11) Xu, W.; Asai, S.; Sumita, M. *Sen'i Gakkaishi* **1997**, *53*, 174−182.
(12) Lagaron, J. M.; Gimenez, E.; Catala, R.; Gavara, R. *Macromol. Chem. Phys.* **2003**, *204*, 704−713.
(13) Zhang, Z.; Britt, I.; Tung, M. *J. Polym. Sci., Part B: Polym. Phys.* **1999**, *37*, 691−699.
(14) Aucejo, S.; Marco, C.; Gavara, R. *J. Appl. Polym. Sci.* **1999**, *74*, 1201.
(15) Lagaron, J. M.; Gimenez, E.; Saura, J. J.; Gavara, R. *Polymer* **2001**, *42*, 9531−9540.
(16) Lagaron, J. M. *J. Mater. Sci.* **2002**, *37*, 4101−4107.
(17) Lagaron, J. M.; Powell, A. K.; Davidson, N. S. *Macromolecules* **2000**, *33*, 1030−1035.

MA035346J